Waveguide Investigations with Millimicrosecond Pulses

By A. C. BECK

(Manuscript received October 11, 1955)

Pulse techniques have been used for many waveguide testing purposes. The importance of increased resolution by means of short pulses has led to the development of equipment to generate, receive and display pulses about 5 or 6 millimicroseconds long. The equipment is briefly described and its resolution and measuring range are discussed. Dominant mode waveguide and antenna tests are described and illustrated. Applications to multimode waveguides are then considered. Mode separation, delay distortion and its equalization, and mode conversion are discussed, and examples are given. The resolution obtained with this equipment provides information that is difficult to get by any other means, and its use has proved to be very helpful in waveguide investigations.

CONTENTS

1. INTRODUCTION

Pulse testing techniques have been employed to advantage in waveguide investigations in numerous ways. The importance of better resolution through the use of short pulses has always been apparent and, from the first, equipment was employed which used as short a pulse as possible. Radar-type apparatus using magnetrons and a pulse width of about one-tenth microsecond has seen considerable use in waveguide research, and many of the results have been published.[1, 2]

To improve the resolution, work was initiated some time ago by S. E. Miller to obtain measuring equipment which would operate with much shorter pulses. As a result, pulses about 5 or 6 millimicroseconds long became available at a frequency of 9,000 mc. In a pulse of this length there are less than 100 cycles of radio frequency energy, and the signal occupies less than ten feet of path length in the transmission medium. The RF bandwidth required is about 500 mc. In order to obtain such bandwidths, traveling wave tubes were developed by J. R. Pierce and members of the Electronics Research Department of the Laboratories. The completed amplifiers were designed by W. W. Mumford. N. J. Pierce, R. W. Dawson and J. W. Bell assisted in the design and construction phases, and G. D. Mandeville has been closely associated in all of this work.

2. PULSE GENERATION

These millimicrosecond pulses have been produced by two different types of generators. In the first equipment, a regenerative pulse generator of the type suggested by C. C. Cutler of the Laboratories was used.[3] This was a very useful device, although somewhat complicated and hard to keep in adjustment. A brief description of it will permit comparisons with a simpler generator which was developed a little later.

A block diagram of the regenerative pulse generator is shown in Fig. 1. The fundamental part of the system is the feedback loop drawn with heavy lines in the lower central part of the figure. This includes a traveling wave amplifier, a waveguide delay line about sixty feet long, a crystal expander, a band-pass filter, and an attenuator. This combination forms an oscillator which produces very short pulses of microwave energy. Between pulses, the expander makes the feedback loop loss too high for oscillation. Each time the pulse circulates around the loop it tends to shorten, due to the greater amplification of its narrower upper part caused by the expander action, until it uses the entire available bandwidth. A 500-mc gaussian band-pass filter is used in the feedback loop of this generator to determine the final bandwidth. An automatic gain control operates with the expander to limit the pulse amplitude, thus preventing amplifier compression from reducing the available expansion.

To get enough separation between outgoing pulses for reflected pulse measurements with waveguides, the repetition rate would need to be too low for a practical delay line length in the loop. Therefore a 12.8-mc fundamental rate was chosen, and a gated traveling wave tube amplifier was used to reduce it to a 100-kc rate at the output. This amplifier is kept in a cutoff condition for 127 pulses, and then a gate pulse restores it to the normal amplifying condition for fifty millimicroseconds, during which time the 128th pulse is passed on to the output of the generator as shown on Fig. 1.

The synchronizing system is also shown on Fig. 1. A 100-kc quartz crystal controlled oscillator with three cathode follower outputs is the basis of the system. One output goes through a seven stage multiplier to get a 12.8-mc signal, which is used to control a pulser for synchronizing the circulating loop. Another output controls the gate pulser for the output traveling wave amplifier. Accurate timing of the gate pulse is obtained by adding the 12.8-mc pulses through a buffer amplifier to the gate pulser. The third output synchronizes the indicator oscilloscope sweep to give a steady pattern on the screen.

Although this equipment was fairly satisfactory and served for many

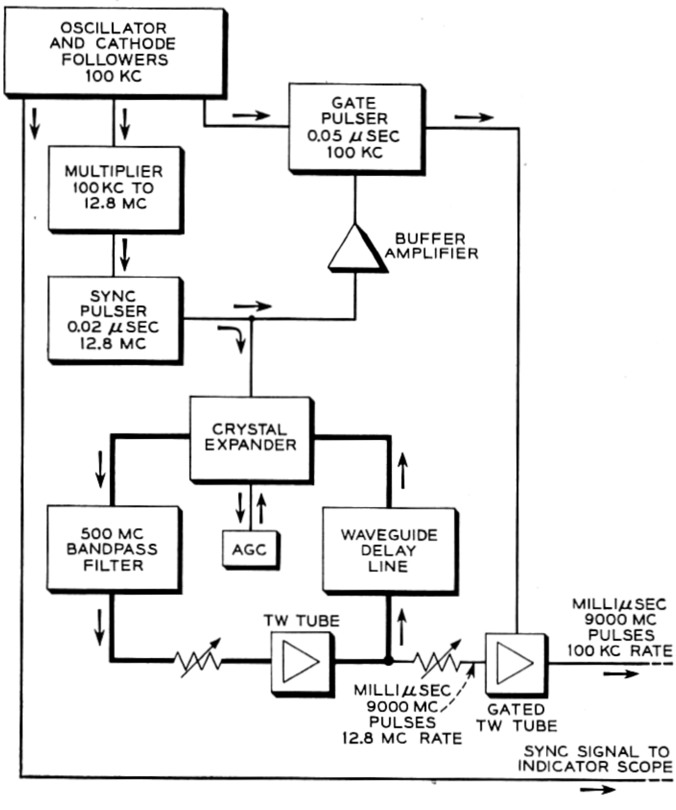

Fig. 1 — Block diagram of the regenerative pulse generator.

testing purposes, it was rather complex and there were some problems in its construction and use. It was difficult to obtain suitable microwave crystals to match the waveguide at low levels in the expander. This would make it even more difficult to build this type of pulse generator for higher frequency ranges. Stability also proved to be a problem. The frequency multiplier had to be very well constructed to avoid phase shift due to drifting. The gate pulser also required care in design and construction in order to get a stable and flat output pulse. It was somewhat troublesome to keep the gain adjusted for proper operation, and the gate pulse time adjustment required some attention. The pulse frequency could not be changed. For these reasons, and in order to get a smaller, lighter and less complicated pulse generator, work was carried out to produce pulses of about the same length by a simpler method.

If the gated output amplifier of Fig. 1 were to have a CW instead of a pulsed input, a pulse of microwave energy would nevertheless appear at the output because of the presence of the gating pulse. This gating pulse is applied to the beam forming electrode of the tube to obtain the gating action. If the beam forming electrode could be pulsed from cutoff to its normal operating potential for a very short time, very short pulses of output energy could be obtained from a continuous input signal. However, it is difficult to obtain millimicrosecond video gating pulses of sufficient amplitude for this purpose at a 100-kc repetition rate.

A traveling-wave tube amplifies normally only when the helix is within a small voltage range around its rated dc operating value. For voltages either above or below this range, the tube is cut off. When the helix voltage is raised through this range into the cutoff region beyond it, and then brought back again, two pulses are obtained, one during a small part of the rise time and the other during a small part of the return time. If the rise and fall times are steep, very short pulses can be obtained. Fig. 2 shows the pulse envelopes photographed from the indicator scope screen when this is done. For the top trace, the helix was biased 300 volts negatively from its normal operating potential, then pulsed to its correct operating range for about 80 millimicroseconds, during which time normal amplification of the CW input signal was obtained. The effect of further increasing the helix video pulse amplitude in the positive direction is shown by the succeeding lower traces. The envelope dips in the middle, then two separated pulses remain — one during a part of the rise time and one during a part of the fall time of helix voltage. The pulses shown on the bottom trace have shortened to about six millimicroseconds in length. The helix pulse had a positive amplitude of about 500 volts for this trace.

Since only one of these pulses can be used to get the desired repetition rate, it is necessary to eliminate the other pulse. This is done in a similar manner to that used for gating out the undesired pulses in the regenerative pulse generator. However, it is not necessary to use another amplifier, as was required there, since the same tube can be used for this purpose, as well as for producing the microwave pulses. Its beam forming electrode is biased negatively about 250 volts with respect to the cathode, and then is pulsed to the normal operating potential for about 50 millimicroseconds during the time of the first short pulse obtained by gating the helix. Thus, the beam forming electrode potential has been returned to the cutoff value during the second helix pulse, which is therefore eliminated.

A block diagram of the resulting double-gated pulse generator is shown in Fig. 3. Comparison with Fig. 1 shows that it is simpler than the regenerative pulse generator, and it has also proved more satisfactory in operation. It can be used at any frequency where a signal source and a traveling-wave amplifier are available, and the pulse

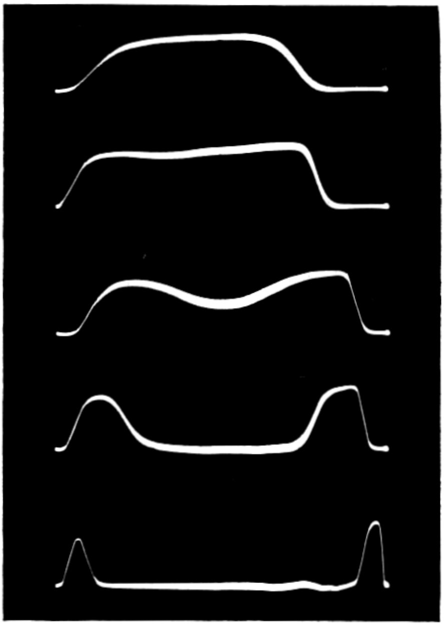

Fig. 2 — Envelopes of microwave pulses at the output of a traveling wave amplifier with continuous wave input and helix gating. The gating voltage is higher for the lower traces.

frequency can be set anywhere within the bandwidth of the traveling-wave amplifier by tuning the klystron oscillator.

The pulse center frequency is shifted from that of the klystron oscillator frequency by this helix gating process. An over-simplified but helpful explanation of this effect can be obtained by considering that the microwave signal voltage on the helix causes a bunching of the electron stream. This bunching has the same periodicity as the microwave signal voltage when the dc helix potential is held constant. However, since the helix voltage is continuously increased in the positive direction during the time of the first pulse, the average velocity of the last bunches of electrons becomes higher than that of the earlier bunches in the pulse, because the later electrons come along at the time of higher positive helix voltage. This tends to shorten the total length of the series of bunches, resulting in a shorter wavelength at the output end of the helix and therefore a higher output microwave frequency. On the second pulse, obtained when the helix voltage returns toward zero, the process is reversed, the bunching is stretched out, and the frequency is decreased. This second pulse is, however, gated out in this arrangement by the beam-forming electrode pulsing voltage. The result for this particular tube and pulse length is an effective output frequency approximately 150 mc higher than the oscillator frequency, but this figure is not constant over the range of pulse frequencies available within the amplifier bandwidth.

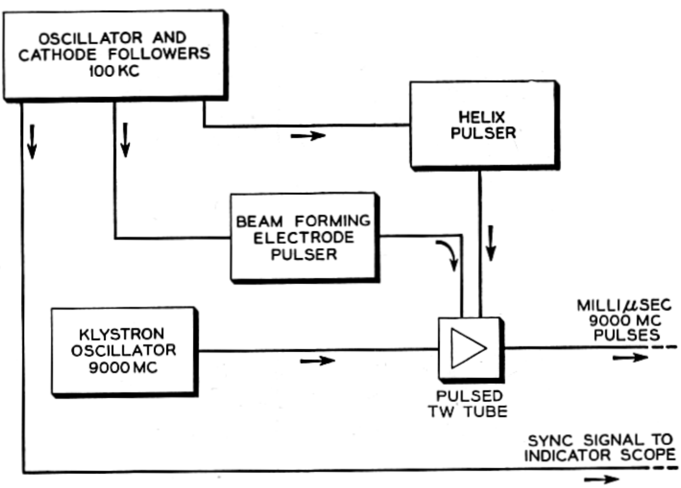

Fig. 3 — Block diagram of the double-gated traveling wave tube millimicrosecond pulse generator.

3. RECEIVER AND INDICATOR

The receiving equipment is shown in Fig. 4. It uses two traveling-wave amplifiers in cascade. A wide band detector and a video amplifier then follow, and the signal envelope is displayed by connecting it to the vertical deflecting plates of a 5 XP type oscilloscope tube. The video amplifier now consists of two Hewlett Packard wide band distributed amplifiers, having a baseband width of about 175 mc. The second one of these has been modified to give a higher output voltage. The sweep circuits for this oscilloscope have been built especially for this use, and produce a sweep speed in the order of 6 feet per microsecond. An intensity pulser is used to eliminate the return trace. These parts of the system are controlled by a synchronizing output from the pulse generator 100-kc oscillator. A precision phase shifter is used at the receiver for the same purpose that a range unit is employed in radar systems. This has a dial, calibrated in millimicroseconds, which moves the position of a pulse appearing on the scope and makes accurate measurement of pulse delay time possible.

Fig. 4 also shows the appearance of the pulses obtained with this equipment. The pulse on the left-hand side of this trace came from the

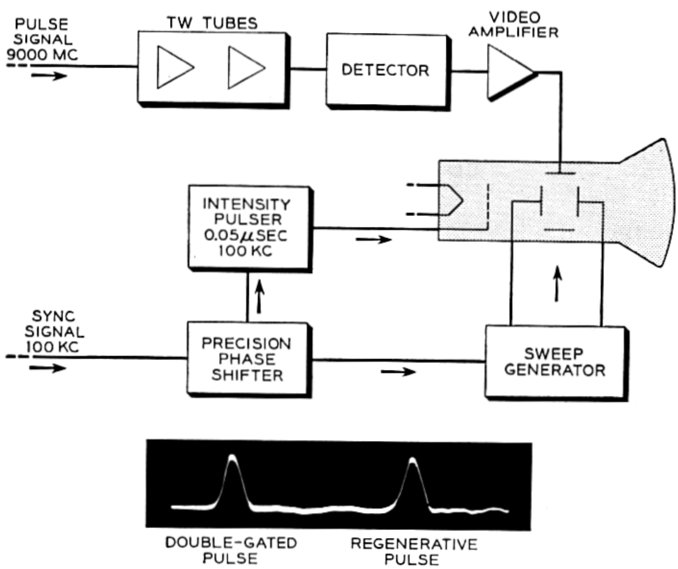

Fig. 4 — Block diagram of millimicrosecond pulse receiver and indicator. The indicator trace photograph shows pulses from each type of generator.

newer double-gated pulse generator, while the pulse on the right was produced by the regenerative pulse generator. It can be seen that they appear to have about the same pulse width and shape. This is partly due to the fact that the video amplifier bandwidth is not quite adequate to show the actual shape, since in both cases the pulses are slightly shorter than can be correctly reproduced through this amplifier. The ripples on the base line following the pulses are also due to the video amplifier characteristics when used with such short pulses.

4. RESOLUTION AND MEASURING RANGE

Fig. 5 shows a piece of equipment which was placed between the pulse generator and the receiver to show the resolution which can be obtained. This waveguide hybrid junction has its branch marked 1 connected to the pulse generator and branch 3 connected to the receiver. If the two side branches marked 2 and 4 were terminated, substantially no energy would be transmitted from the pulser straight through to the receiver. However, a short circuit placed on either side branch will send energy through the system to the receiver. Two short circuits were so placed that the one on branch 4 was 4 feet farther away from the hybrid junction than the one on branch 2. The pulse appearing first is produced by a signal traveling from the pulse generator to the short circuit on branch 2 and then through to the receiver, as shown by the path drawn with short dashes. A second pulse is produced by the signal which travels

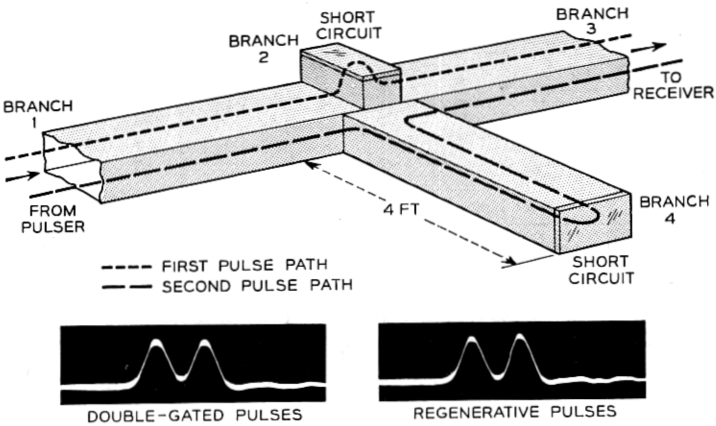

Fig. 5 — Waveguide hybrid circuit used to demonstrate resolution of millimicrosecond pulses. Trace photographs of pulses from each type of generator are shown.

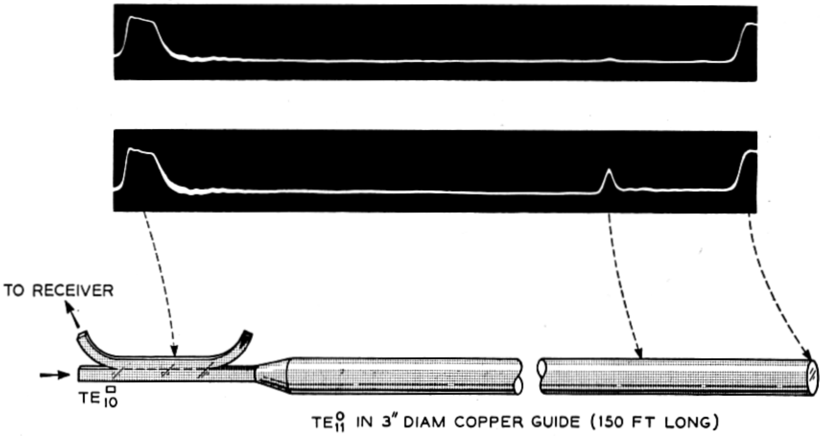

Fig. 6 — Waveguide arrangement and oscilloscope trace photos showing presence and location of defective joint. The dominant mode (TE_{11}) was used with its polarization changed 90 degrees for the two trace photos.

from the pulse generator through branch 4 to the short circuit and then to the receiver as shown by the long dashed line. This pulse has traveled 8 feet farther in the waveguide than the first pulse. This would be equivalent to seeing separate radar echoes from two targets about 4 feet apart. Resolution tests made in this way with the pulses from the regenerative pulse generator, and from the double-gated pulse generator, are shown on Fig. 5. With our video amplifier and viewing equipment, there is no appreciable difference in the resolution obtained using either type of pulse generator.

The measuring range is determined by the power output of the gated amplifier at saturation and by the noise figure of the first tube in the receiver. In this equipment the saturation level is about 1 watt, and the noise figure of the first receiver tube is rather poor. As a result, received pulses about 70 db below the outgoing pulse can be observed, which is enough range for many measurement purposes.

5. DOMINANT MODE WAVEGUIDE TESTS

Fig. 6 shows the use of this equipment to test 3″ round waveguides such as those installed between radio repeater equipment and an antenna. This particular 150-foot line had very good soldered joints and was thought to be electrically very smooth. The signal is sent in through a transducer to produce the dominant TE_{11} mode. The receiver is connected through a directional coupler on the sending end to look for any

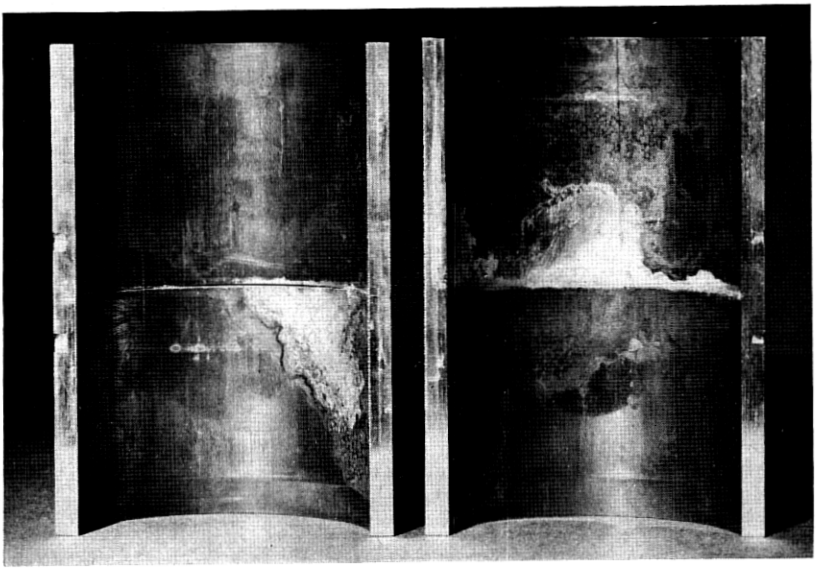

Fig. 7 — Defective joint caused by imperfect soldering which gave the reflection shown on Fig. 6.

reflections from imperfections in the line. The overloaded signal at the left of the oscilloscope trace is produced by leakage directly through the directional coupler. The overloaded signal on the other end of this trace is produced by the reflection from the short circuit piston at the far end of the waveguide. The signal between these two, which is about 45 db down from the input signal, is produced by an imperfect joint in the waveguide. The signal polarization was oriented so that a maximum reflection was obtained in the case of the lower trace. In the other trace, the polarization was changed by 90°. It is seen that this particular joint produces a stronger reflection for one polarization than for the other. By use of the precision phase shifter in the receiver the exact location of this defect was found and the particular joint that was at fault was sawed out. Fig. 7 shows this joint after the pipe had been cut in half through the middle. The guide is quite smooth on the inside in spite of the discoloration of some solder that is shown here, but on the left-hand side of the illustration the open crack is seen where the solder did not run in properly. This causes the reflected pulse that shows on the trace. The fact that this crack is less than a semi-circumference in length causes the echo to be stronger for one polarization than for the other.

Fig. 8 shows the same test for a 3″ diameter aluminum waveguide 250 feet long. This line was mounted horizontally in the test building with compression couplings used at the joints. The line expanded on warm days but the friction of the mounting supports was so great that it pulled open at some of the joints when the temperature returned to normal. These open joints produced reflected pulses from 40 to 50 db down, which are shown here. They come at intervals equal to the length of one section of pipe, about 12 feet. Some of these show polarization effects where the crack was more open on one side than on the other, but others are almost independent of polarization. These two photographs of the trace were taken with the polarization changed 90°.

Fig. 9 shows the same test for a 3″ diameter galvanized iron waveguide. This line had shown fairly high loss using CW for measurements. The existence of a great many echoes from random distances indicates a rough interior finish in the waveguide. Fig. 10 shows the kind of inperfections in the zinc coating used for galvanizing which caused these reflections.

6. TESTING ANTENNA INSTALLATIONS

The use of this equipment in testing waveguide and antenna installations for microwave radio repeater systems is shown in Fig. 11. This particular work was done in cooperation with A. B. Crawford's antenna research group at Holmdel, who designed the antenna system. A directional coupler was used to observe energy reflections from the system under test. In this installation a 3″ diameter round guide carrying the TE_{11} mode was used to feed the antenna. Two different waveguide

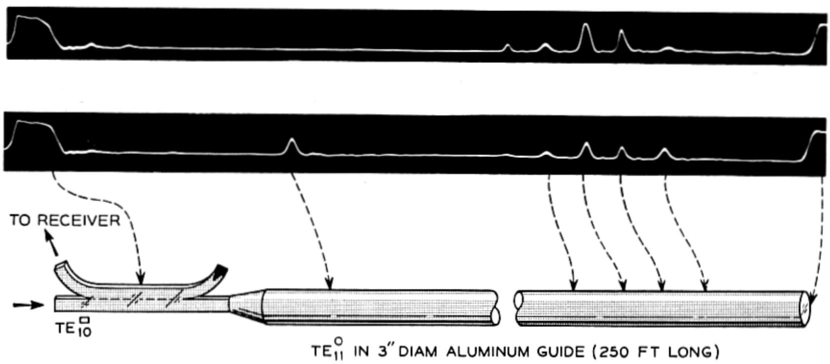

Fig. 8 — Reflections from several defective joints in a dominant (TE_{11}) mode waveguide. The two trace photos are for polarizations differing by 90 degrees.

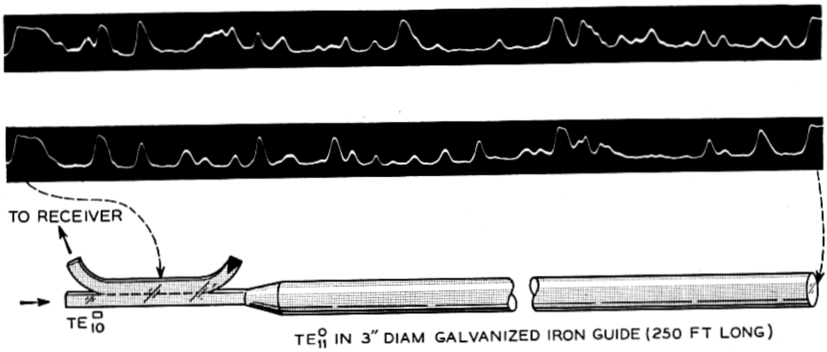

Fig. 9 — Multiple reflections from a dominant (TE_{11}) mode waveguide with a rough inside surface. The two trace photos are for polarizations differing by 90 degrees.

joints are shown here. In addition, a study was being made of the return loss of the transition piece at the throat of the antenna which connected the 3″ waveguide to the square section of the horn. The waveguide sections are about 10 feet long. The overloaded pulse at the left on the traces is the leakage through the directional coupler. The

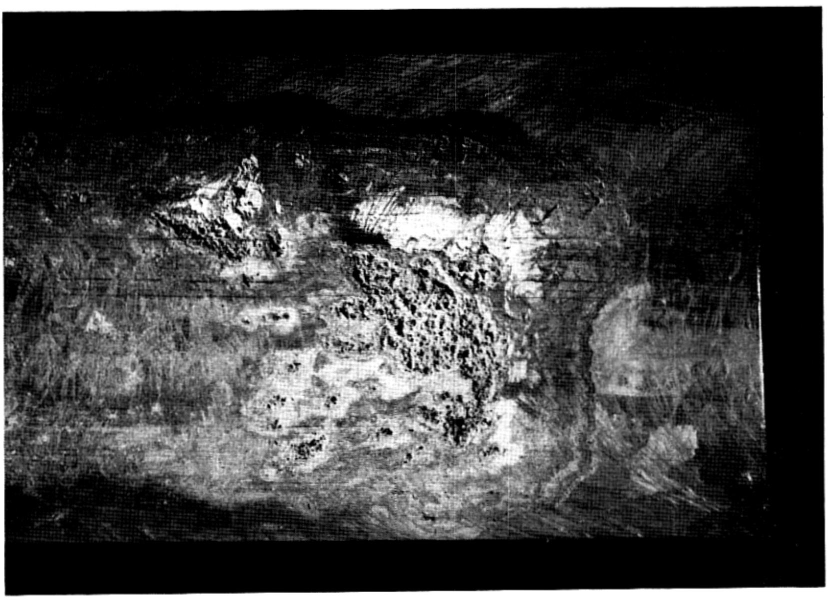

Fig. 10 — Rough inside surface of a galvanized iron waveguide which produced the reflections shown on Fig. 9.

other echoes are associated with the parts of the system from which they came by the dashed lines and arrows on the figure. A clamped joint in the line gave the reflection shown next following the initial overloaded pulse. A well made threaded coupling in which the ends of the pipe butted squarely is seen to have a very much lower reflection, scarcely observable on this trace. Since there is always reflection from the mouth and upper reflector parts of this kind of antenna, it is not possible to measure a throat transition piece alone by conventional CW methods, as the total reflected power from the system is measured. Here, use of the resolution of this short pulse equipment completely separated the reflection of the transition piece from all other reflections and made a measurement of its performance possible. In this particular case, the reflection from the transition is more than 50 db down from the incident signal which represents very good design. As can be seen,

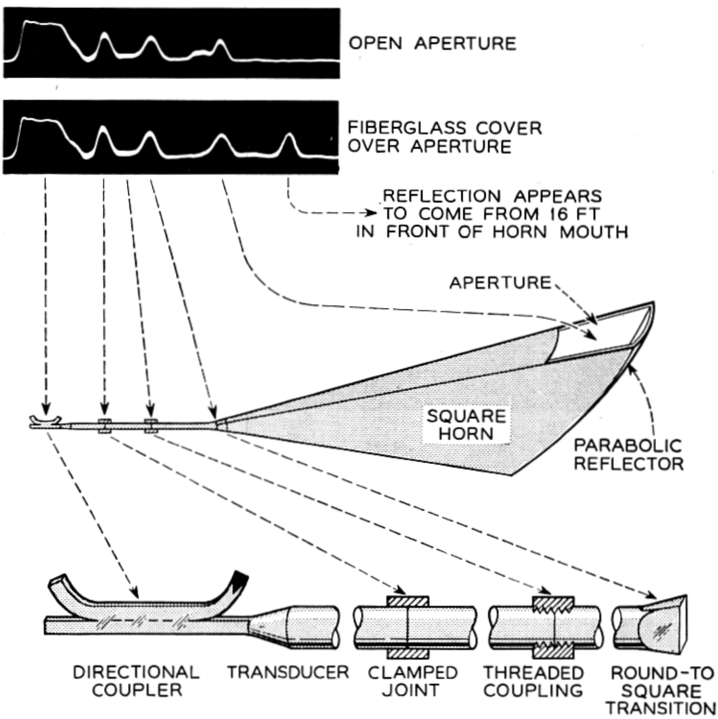

Fig. 11 — Waveguide and antenna arrangement with trace photos showing reflections from joints, transition section, and cover.

the reflection from the parabolic reflector and mouth is also quite low, and this characterizes a good antenna installation.

The extra reflected pulse on the right of the lower trace on Fig. 11 appeared when a fiberglas weatherproof cover was installed over the open mouth of the horn. This cover by itself would normally produce a troublesome reflection. However, in this antenna, it is a continuation of one of the side walls of the horn. Consequently, outgoing signals strike it at an oblique angle. Reflected energy from it is not focused by the parabolic section back at the waveguide, so the overall reflected power in the waveguide was found to be rather low. However, measuring it with this equipment, we found that an extra reflection appeared to come from a point 16 feet out in front of the mouth of the horn when the cover was in place. This is accounted for by the fact that energy reflected obliquely from this cover bounces back and forth inside the horn before getting back into the waveguide, thus traveling the extra distance that makes the measurement seem to show that it comes from 16 feet out in front.

7. SEPARATION OF MODES ON A TIME BASIS

If a pulse of energy is introduced into a moderate length of round waveguide to excite a number of modes which travel with different group velocities, and then observed farther along the line, or reflected from a piston at the end and observed at the beginning, separate pulses will be seen corresponding to each mode that is sent. This is illustrated

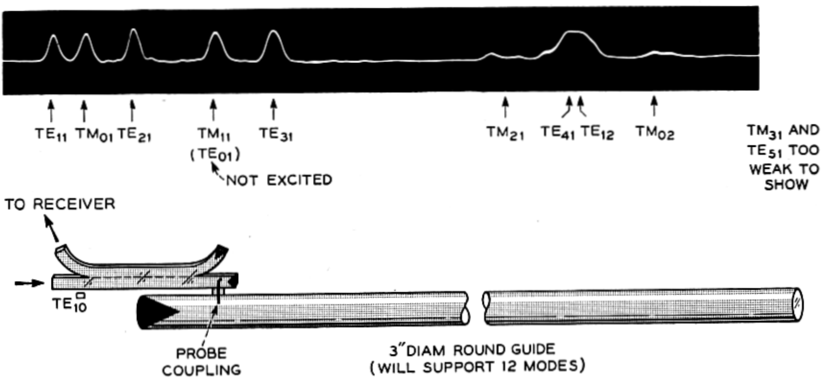

Fig. 12 — Arrangement for showing mode separation on a time basis in a multimode waveguide. The pulses in the trace photo have all traveled to the piston and back. The earlier outgoing pulse due to directional coupler unbalance is not shown.

in Fig. 12. In this arrangement energy was sent into the round line from a probe inserted in the side of the guide. This couples to all of the 12 modes which can be supported, with the exception of the TE_{01} circular electric mode. The sending end of the round guide was terminated. A directional coupler is connected to the sending probe so that the return from the piston at the far end can be observed on the receiver. Because of the different time that each mode takes to travel one round trip in this waveguide, which was 258 feet long, separate pulses are seen for each mode. The pulses in this figure have been marked to show which mode is being received.

The time of each pulse referred to the outgoing pulse was measured and found to check very well with the calculated time. The formula for the time of transit in the waveguide for any mode is:

$$T = \frac{L}{0.98322\sqrt{1 - v_{nm}^2}}$$

where T = time in millimicroseconds

L = length of pulse travel in feet

$v_{nm} = \lambda/\lambda_c$

λ = operating wavelength in air

λ_c = cutoff wavelength of guide for the mode involved.

TABLE I — CALCULATED AND MEASURED VALUE OF TIME FOR ONE ROUND TRIP

Mode Number	Mode Designation	Time in Millimicroseconds	
		Calculated	Measured
1	TE_{11}	545	545
2	TM_{01}	561	561
3	TE_{21}	587	587
4	TM_{11}	634	634
5	TE_{01}	634	—
6	TE_{31}	665	665
7	TM_{21}	795	793
8	TE_{41}	835	838
9	TE_{12}	838	—
10	TM_{02}	890	890
11	TM_{31}	1461	—
12	TE_{51}	1519	—

The calculated and measured value of time for one round trip is given in Table I.

In this experiment the operating wavelength was 3.35 centimeters. This was obtained by measurements based on group velocity in a number of guides as well as information about the pulse generator components. It represents an effective wavelength giving correct time of travel. The pulse occupies such a wide bandwidth that a measurement of its wavelength is difficult by the usual means.

The dashes in the measured column indicate that the mode was not excited by the probe or was too weak to measure. These modes do not appear on the oscilloscope trace photograph.

The relative pulse heights can be calculated from a knowledge of the probe coupling factors and the line loss. The probe coupling factors as given by M. Aronoff in unpublished work are expressed by the following:

For TE_{nm} modes:

$$P = 2.390 \frac{n^2}{K_{nm}^2 - n^2} \frac{\lambda_{gnm}}{\lambda_{g11}}$$

For TM_{nm} modes:

$$P = 1.195\epsilon_n \frac{\lambda}{\lambda_{g11}} \frac{\lambda}{\lambda_{gnm}}$$

where

P = ratio of probe coupling power in mode nm to that in mode TE_{11}

n = first index of mode being calculated

K_{nm} = Bessel function zero value for mode being calculated $= \pi d/\lambda_c$

λ = wavelength in air

λ_g = wavelength in the guide for the mode involved

λ_c = cutoff wavelength of guide for the mode involved

$\epsilon_n = 1$ for $n = 0$

$\epsilon_n = 2$ for $n \neq 0$

d = waveguide diameter

Formulas for guide loss as given by S. A. Schelkunoff on page 390 of his book *Electromagnetic Waves* for this case where the resistivity of the aluminum guide is 4.14×10^{-6} ohms per cm cube are:

For TE_{nm} modes:

$$\alpha = 3.805\left(\frac{n^2}{K_{nm}^2 - n^2} + v_{nm}^2\right)(1 - v_{nm}^2)^{-1/2}$$

For TM_{nm} modes:

$$\alpha = 3.805(1 - v_{nm}^2)^{-1/2}$$

where:

α = attenuation of this aluminum guide in db

n = first index of mode being calculated

K_{nm} = Bessel function zero value for mode being calculated $= \pi d/\lambda_c$

$v_{nm} = \lambda/\lambda_c$

λ = operating wavelength in air

λ_c = cutoff wavelength of guide for the mode involved

d = waveguide diameter

Table II gives the calculated probe coupling factor, line loss, and relative pulse height for each mode. In the calculation of the latter, wave ellipticity and loss due to mode conversion were neglected, but the heat loss given by the preceding formulas has been increased 20 per cent for all modes, to take account of surface roughness. Relative pulse heights were obtained by subtracting the relative line loss from twice the relative probe coupling factor. The relative line loss is the number in the table minus 2.33 db, the loss for the TE_{11} mode.

The actual pulse heights on the photo of the trace on Fig. 12 are in fair agreement with these calculated values. Differences are probably due to polarization rotation in the guide (wave ellipticity) and conversion to other modes, effects which were neglected in the calculations, and which are different for different modes.

Calculated pulse heights with this guide length, except for modes near cutoff, vary less than the probe coupling factors, because line loss is high when tight probe coupling exists. This is to be expected, since both are the result of high fields near the guide walls.

The table of round trip travel time shows that the TE_{41} and TE_{12} modes are separated by only three millimicroseconds after the round trip in this waveguide. They would not be resolved as separate pulses by this equipment. However, the table of calculated pulse heights shows that the TE_{41} pulse should be about 22 db higher than the TE_{12} pulse.

TABLE II — CALCULATED PROBE COUPLING FACTOR, LINE LOSS AND PULSE HEIGHT FOR EACH MODE

Mode Number	Mode Designation	Relative Probe Coupling Factor, db	1.2 × Theoretical Line Loss, db	Calculated Relative Pulse Heights, db
1	TE_{11}	0	2.33	0
2	TM_{01}	+0.32	4.88	−1.91
3	TE_{21}	+2.86	4.85	+3.20
4	TM_{11}	+2.80	5.51	+2.42
5	TE_{01}	−∞	1.73	−∞
6	TE_{31}	+4.82	8.21	+3.76
7	TM_{21}	+1.82	6.92	−0.95
8	TE_{41}	+6.80	13.86	+2.07
9	TE_{12}	−8.73	4.70	−19.83
10	TM_{02}	−1.68	7.74	−8.77
11	TM_{31}	−0.82	12.71	−12.02
12	TE_{51}	+10.14	32.09	−9.48

Since the TE_{12} pulse is so weak, it would not show on the trace even if it were resolved on a time basis. Coupling to the TM_{02} mode is rather weak, and the gain was increased somewhat at its position on the trace to show its time location.

8. DELAY DISTORTION

Another effect of the wide bandwidth of the pulses used with this equipment can be observed in Fig. 12. The pulses that have traveled for a longer time in the guide are in the modes closer to cutoff, and are on the right-hand side of the oscilloscope trace. They are broadened and distorted compared with the ones on the left-hand side. This effect is due to delay distortion in the guide. This can be explained by reference to Fig. 13. On this figure the ratio of group velocity to the velocity in an unbounded medium is shown plotted as a function of frequency for each of the modes that can be propagated. The bandwidth of the transmitted pulse is indicated by the vertical shaded area. It will be noticed that the spacing of the pulses on the oscilloscope trace on Fig. 12 from left to right in time corresponds to the spacing of the group velocity curves in the bandwidth of the pulse from top to bottom. Delay distortion on these curves is shown by the slope of the line across the pulse bandwidth. If the line were horizontal, showing the same group velocity at all points in the band, there would be no delay distortion. The greater the difference in group velocity at the two edges of the band, the greater the delay distortion. The curves of Fig. 13 indicate that there should be increasing amounts of delay distortion reading from top to bottom for the pulse bandwidth used in these experiments. The effect of this delay distortion is to cause a broadening of the pulse. Examination of the pulse pattern of Fig. 12 shows that the later pulses corresponding in mode designation to the lower curves of Fig. 13 do indeed show a broadening due to the increased delay distortion. One method of reducing the effect of delay distortion is to use frequency division multiplex so that each signal uses a smaller bandwidth. Another way, suggested by D. H. Ring, is to invert the band in a section of the waveguide between one pair of repeaters compared with that between an adjacent pair of repeaters so that the slope is, in effect, placed in the opposite direction, and delay distortion tends to cancel out, to a first order at least.

The quantitative magnitude of delay distortion has been expressed by S. Darlington in terms of the modulating base-band frequency needed to generate two side frequencies which suffer a relative phase error of 180° in traversing the line. This would cause cancellation of a single frequency AM signal, and severe distortion using any of the

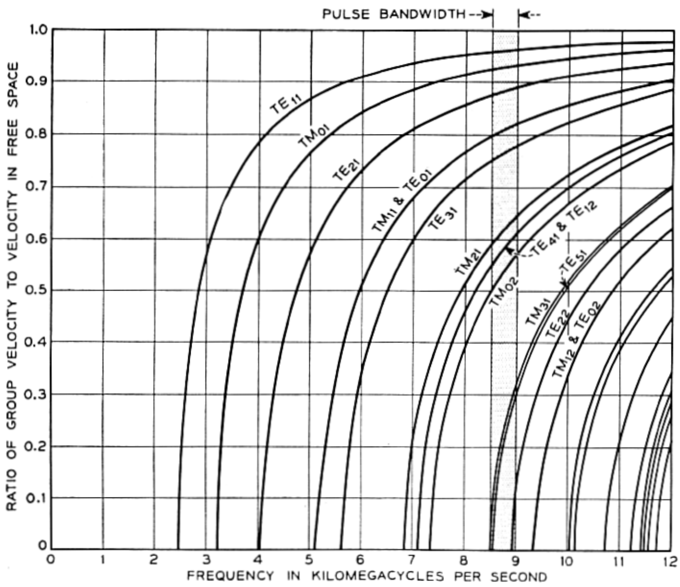

Fig. 13 — Theoretical group velocity vs. frequency curves for the 3″ diameter waveguide used for the tests shown on Fig. 12. The vertical shaded area gives the bandwidth for the millimicrosecond pulses employed in that arrangement.

ordinary modulation methods. Darlington gives this formula:

$$fB = f\left(\frac{\lambda}{2L}\right)^{1/2} \frac{(1 - v_{nm}^2)^{3/4}}{v_{nm}}$$

where:

fB = base bandwidth for 180° out of phase sidebands

f = operating frequency (in same units as fB)

λ = wavelength in air

L = waveguide length (in same units as λ)

v_{nm} = λ/λ_c

λ_c = cutoff wavelength for the mode involved

With this equipment, the base bandwidth of the pulse is about 175 mc, and when fB from the formula above is about equal to or less than this, pulse distortion should be observed. The following Table III gives fB calculated from this formula for the arrangement shown on Fig. 12.

It is interesting to note that pulses in the TM_{11} and TE_{31} modes, for which fB is less than the 175-mc pulse bandwidth, are broadened, but not badly distorted. For the higher modes, where fB is much less than 175 mc, broadening and severe distortion are evident. Another example is given in the next section.

9. DELAY DISTORTION EQUALIZATION

If the distance which a pulse travels in a waveguide is increased, its delay distortion also increases. Since the group velocity at one edge of the band is different than at the other edge of the band, the amount by which the two edges get out of phase with each other increases with the total length of travel, causing increased distortion and pulse broadening. The Darlington formula in the previous section shows that fB varies inversely as the square root of the length of travel. This effect is shown on Fig. 14. In this arrangement the transmitter was connected to the end of a 3″ diameter round waveguide 107 feet long through a small hole in the end plate. A mode filter was used so that only the TE_{01} mode would be transmitted in this waveguide. Through another small hole in the end plate polarized 90° from the first one, and rotated 90° around the plate, a directional coupler was connected as shown. The direct through guide of this directional coupler could be short circuited with a waveguide shorting switch. Energy reflected from this

Table III — Calculated Values of fB for the Arrangement Shown in Fig. 12

Mode Number	Mode Designation	fB Megacycles	Remarks
1	TE_{11}	324.0	
2	TM_{01}	237.7	
3	TE_{21}	174.9	
4	TM_{11}	124.1	
5	TE_{01}	124.1	Not excited
6	TE_{31}	105.2	
7	TM_{21}	65.9	
8	TE_{41}	59.1	
9	TE_{12}	58.6	Very weakly excited
10	TM_{02}	51.8	
11	TM_{31}	21.3	Not observed
12	TE_{51}	20.0	Not observed

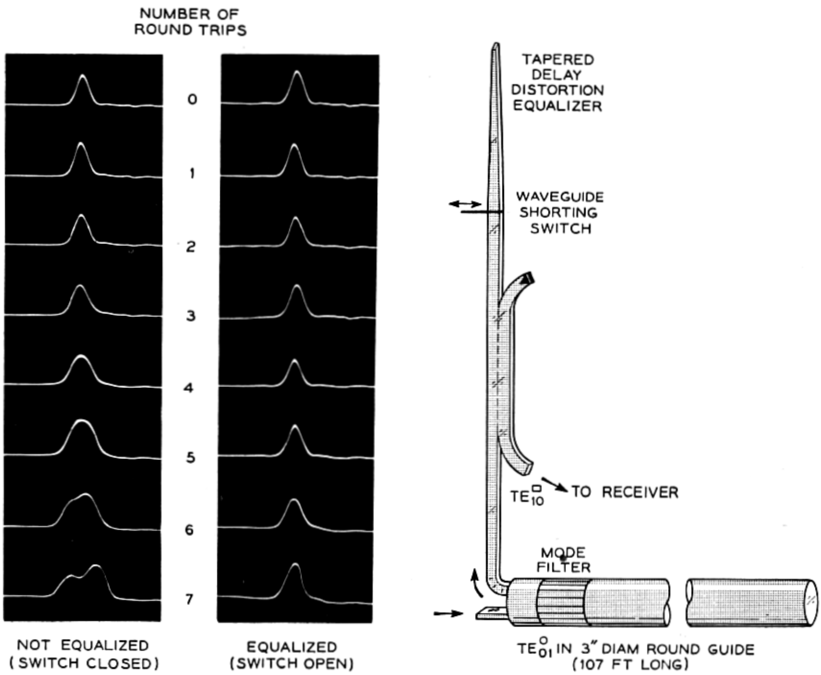

Fig. 14 — The left-hand series of pulses shows the build up of delay distortion with increasing number of round trips in a long waveguide. The right-hand series shows the improvement obtained with the tapered delay distortion equalizer shown at the right.

switch was then taken through the directional coupler to the receiver as shown by the output arrow. The series of pulses at the left-hand photograph of the oscilloscope traces was taken with this waveguide shorting switch closed. The top pulse shows the direct leakage across the inside of the end plate before it has traveled through the 3″ round guide. The next pulse is marked one round trip, having gone therefore 214 feet in the TE_{01} mode in the round waveguide. The successive pulses have traveled more round trips as shown by the number in the center between the two photographs. The effect of increased delay distortion broadening and distorting the pulse can be seen as the numbers increase. The values of fB from the Darlington formula in the previous section for these lengths are given in Table IV.

It will be noticed that pulse broadening, and eventually severe distortion, occurs as fB decreases much below the 175-mc pulse bandwidth. The effect is gradual, and not too bad a pulse shape is seen until fB is about half the pulse bandwidth, although broadening is very evident earlier.

When the waveguide short-circuiting switch was opened so that the tapered delay distortion equalizer was used to reflect the energy, instead of the switch, the series of pulses at the right was observed on the indicator. It will be noted that there is much less distortion of these pulses, particularly toward the bottom of the series. The ones at the top have less distortion than would be expected, probably because of frequency modulation of the injected pulse. The equalizer consists of a long gradually tapered section of waveguide which has its size reduced to a point beyond cutoff for the frequencies involved. Reflection takes place at the point of cutoff in this tapered guide. For the high frequency part of the pulse bandwidth, this point is farther away from the shorting switch than for the low frequency part of the bandwidth. Consequently, the high frequency part of the pulse travels farther in one round trip into this tapered section and back than the low frequency part of

Table IV — Values of fB from the Darlington Formula for the Arrangement Shown in Fig. 14

Round Trip Number	fB Megacycles	Round Trip Number	fB Megacycles
1	185.8	6	75.8
2	131.4	7	70.2
3	107.3	8	65.7
4	92.9	9	61.9
5	83.1	10	58.7

the pulse. This increased time of travel compensates for the shorter time of travel of the high frequency edge of the band in the 3″ round waveguide, so equalization takes place. Since this waveguide close to cutoff introduces considerable delay distortion by itself, the taper effect must be made larger in order to secure the equalization. This can be done by making the taper sufficiently gradual. This type of equalizer introduces a rather high loss in the system. For this reason it might be used to predistort the signal at an early level in a repeater system. Equalization by this method was suggested by J. R. Pierce.

10. MEASURING MODE CONVERSION FROM ISOLATED SOURCES

One of the important uses of this equipment has been for the measurement of mode conversion. W. D. Warters has cooperated in developing techniques and carrying out such measurements. One of the problems in the design of mode filters used for suppressing all modes except the circular electric ones in round multimode guides is mode conversion. Since these mode filters have circular symmetry, conversion can take place only to circular electric modes of order higher than the TE_{01} mode. This conversion is, however, a troublesome one, since these higher order circular modes cannot be suppressed by the usual type of filter.

An arrangement for measuring mode conversion at such mode filters from the TE_{01} to the TE_{02} mode is being used with the short pulse equipment. This employs a 400-foot long section of the 5″ diameter line. Because the coupled-line transducer available had too high a loss to TE_{02}, a combined TE_{01} — TE_{02} transducer was assembled. It uses one-half of the round waveguide to couple to each mode. Fig. 15 shows this device.

The use of this transducer and line is illustrated in Fig. 16. Pulses in the TE_{01} mode are sent into the waveguide by the upper section of the transducer as shown. Some of the TE_{01} energy goes directly across to the TE_{02} transducer and appears as the outgoing pulse with a level down about 32 db. This is useful as a time reference in the system and is shown as the outgoing pulse in the photo of the oscilloscope trace above. The main energy in the TE_{01} mode propagates down the line as shown by dashed line 2, which is the path of this wave. Most of this energy goes all the way to the reflecting piston at the far end and then returns to the TE_{02} transducer where it gives a pulse which is marked TE_{01} round trip on the trace photograph above. Two thirds of the way from the sending end to the piston, the mode filter being measured is inserted in the line. When the TE_{01} mode energy comes to this mode filter, a small amount of it is converted to the TE_{02} mode. This

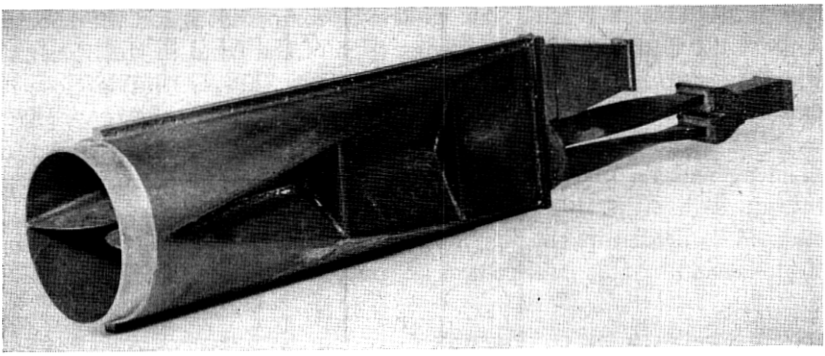

Fig. 15 — A special experimental transducer for injecting the TE_{01} mode and receiving the converted TE_{02} mode in a 5″ diameter waveguide.

continues to the piston by path 4 (with dashed lines and crosses) and then returns and is received by the TE_{02} part of the transducer. This appears on the trace photo as the TE_{02} first conversion. When the main TE_{01} energy reflected by the piston comes back to the mode filter, conversion again takes place to TE_{02}. This is shown by path 3 having dashed lines and circles. This returns to the TE_{02} part of the transducer and appears on the trace photo as the TE_{02} second conversion. In addition, a small amount of energy in the TE_{02} mode is generated by the TE_{01} upper part of the transducer. It is shown by path 5, having

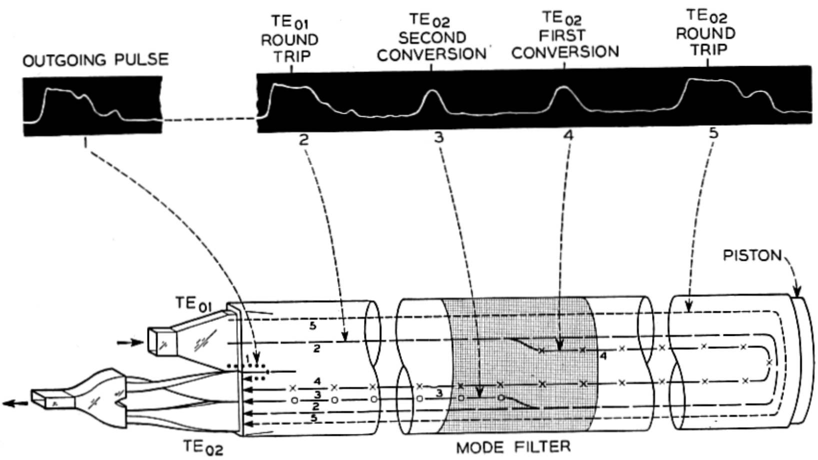

Fig. 16 — Trace photos and waveguide paths traveled when measuring TE_{01} to TE_{02} mode conversion at a mode filter with the transducer shown on Fig. 15.

short dashes. This goes down through the waveguide to the far end piston and back, and is received by the TE_{02} transducer and shown as the pulse marked TE_{02} round trip. The pulse marked TE_{01} round trip has a time separation from the outgoing pulse which is determined by the group velocity of TE_{01} waves going one round trip in the guide. The TE_{02} round trip pulse appears at a time corresponding to the group velocity of the TE_{02} mode going one round trip in the guide. Spacing the mode filter two-thirds of the way down produces the two conversion pulses equally spaced between these two as shown in Fig. 16. The first conversion pulse appears at a time which is the sum of the time taken for the TE_{01} to go down to the filter and the TE_{02} to go from the filter to the piston and back to the receiver. Because of the slower velocity of the TE_{02}, this appears at the time shown, since it was in the TE_{02} mode for a longer time than it was in the TE_{01} mode. The second conversion, which happened when TE_{01} came back to the mode filter, comes earlier in time than the first conversion, since the path for this signal was in the TE_{01} mode longer than it was in the TE_{02} mode. This arrangement gives very good time separation, and makes possible a measurement of the amount of mode conversion taking place in the mode filters. Mode conversion from TE_{01} to TE_{02} as low as 50 to 55 db down, can be measured with this equipment.

Randomly spaced single discontinuities in long waveguides can be located by this technique if they are separated far enough to give individually resolved short pulses in the converted mode. Fig. 17 shows

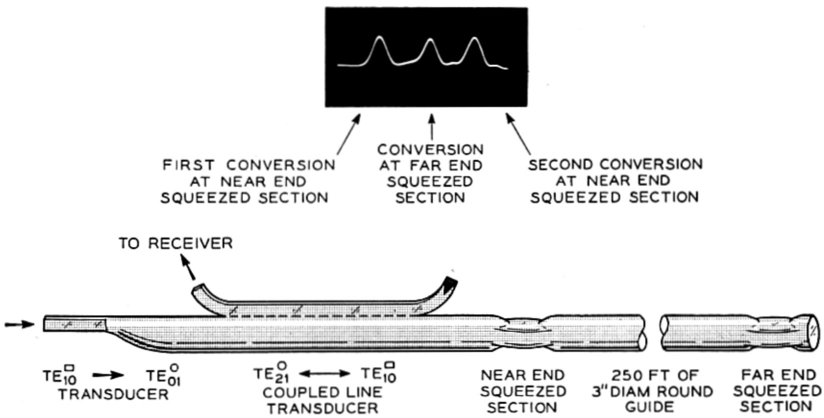

Fig. 17 — Arrangement used to explain the measurement and location of mode conversion from isolated sources. A deliberately squeezed section was placed at each end of the long waveguide, producing the pulses shown in the trace photo.

an arrangement having oval sections deliberately placed in the waveguide in order to explain the method. Pure TE_{01} excitation is used, and the converted TE_{21} mode observed with a coupled line transducer giving an output for that mode alone.

Let us consider first what would happen with the far-end squeezed section alone, omitting the near-end squeezed section from consideration. The injected TE_{01} mode signal would then travel down the 250 feet of 3″ diameter round waveguide to the far end with substantially no mode conversion at the level being measured. At this point it goes through the squeezed section. Conversion now takes place from the TE_{01} mode to the TE_{21} mode. Both these modes after reflection from the piston travel back up the waveguide to the sending end. The group velocity of the TE_{21} mode is higher than the group velocity of the TE_{01} mode, so energy in these two modes separates, and if a coupling system were used to receive energy in both modes, two pulses would appear, with a time separation between them. In this case, since the receiver is connected to the line through the coupled line transducer which is responsive only to the TE_{21} mode, only one pulse is seen, that due to this mode alone. This is the center pulse in the trace photograph at the top of Fig. 17. If only one mode conversion point at the far end of the guide exists, only this one pulse is seen at the receiver. It would be spaced a distance away from the injected outgoing pulse that corresponds in time to one trip of the TE_{01} mode down to the far end and one trip of the TE_{21} mode from the far end back to the receiver.

Now let us consider what would happen if the near-end squeezed section alone were present. When the TE_{01} wave passes the oval section just beyond the coupled line transducer, conversion takes place, and the energy travels down the line in both the TE_{01} and the TE_{21} modes, at a higher group velocity in the TE_{21} mode. These two signals are reflected by the piston at the far end and return to the sending end. The TE_{21} signal comes through the coupled line transducer and appears as the pulse at the left of the photo shown on Fig. 17. Now the TE_{01} energy has lagged behind the TE_{21} energy, and when it gets back to the near-end squeezed section, a second mode conversion takes place, and TE_{21} mode energy is produced which comes through the coupled line transducer and appears at the receiver at the time of the right hand pulse. The spacing between these two pulses is equal to the difference in round trip times between the two modes.

In general, for a single conversion source occurring at any point in the line, two pulses will appear on the scope. The spacing between these pulses corresponds to the difference in group velocity between the modes from the point of the discontinuity down to the piston at the far end, and then back to the discontinuity. If the discontinuity is at the far end, this time difference becomes zero, and a single pulse is seen. By making a measurement of the pulse spacing, the location of a single conversion point can be determined.

In the arrangement illustrated in Fig. 17, two isolated sources of conversion existed. They were spaced far enough apart so that they were resolved by this equipment, and all three pulses were observed. The two outside pulses were due to the first conversion point. The center pulse was caused by the other squeeze, which was right at the reflecting piston. If this conversion point had been located back some distance from the piston, it would have produced two conversion pulses whose spacing could be used to determine the location of the conversion point.

The coupled-line transducers are calibrated for coupling loss by sending the pulse through a directional coupler into the branch normally used for the output to the receiver. This gives a return loss from the directional coupler equal to twice the transducer loss plus the round trip line loss.

11. MEASURING DISTRIBUTED MODE CONVERSION IN LONG WAVEGUIDES

Measurements of mode conversion from TE_{01} to a number of other modes have been made with 5″ diameter guides using this equipment. The arrangement of Fig. 18 was set up for this purpose. This is the same as Fig. 17, except that a long taper was used at the input end of the 5″ waveguide, and a movable piston installed at the remote end.

One of the converted modes studied with this apparatus arrangement was the TM_{11} mode, which is produced by bends in the guide. This mode has the same velocity in the waveguide as the TE_{01} mode. Therefore energy components converted at different points in the line stay in phase with the injected TE_{01} mode from which they are converted. There is never any time separation between these modes, and a single

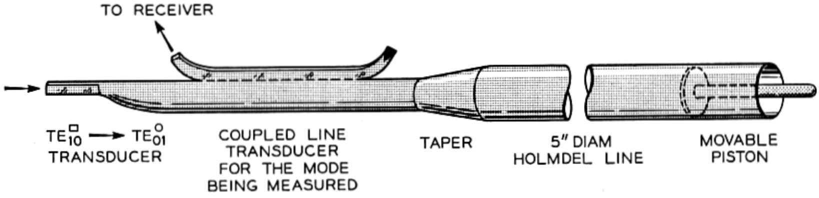

Fig. 18 — Arrangement used for measuring mode conversion in the 5″ diameter waveguides at Holmdel.

narrow pulse like the transmitted one is all that appears on the indicator oscilloscope. It is not possible from this to get any information about the location or extent of the conversion points in the line. Moving the far end piston does not change the relative phases of the modes, so no changes are seen in indicator pattern or pulse level as the piston is moved. For the Holmdel waveguides, which are about 500 feet long, the total round trip TM_{11} mode converted level varies from 32 to 36 db below the input TE_{01} mode level over a frequency range from 8,800 to 9,600 mc per second.

All the other modes have velocities that are different than that of the TE_{01} mode. When mode conversion takes place at many closely spaced points along the waveguide, the pulses from the various sources overlap, and phasing effects take place. In general, a filled-in pulse much longer than the injected one is observed. The maximum possible, but not necessary, pulse length is equal to the difference in time required for the TE_{01} mode and the converted mode to travel the total waveguide length being observed. The phasing effects within the broadened pulse change its height and shape as a function of frequency and line length.

Measurements of mode conversion from TE_{01} to TE_{31} in these waveguides illustrate distributed sources and piston phasing effects. The TE_{31} mode has a group velocity 1.4 per cent slower than the TE_{01} mode. For a full round trip in the 500-foot lines, assuming conversion at the imput end, this causes a time separation of about two and one half pulse widths between these two modes. The received pulse is about two and a half times as long as the injected pulse, indicating rather closely spaced sources over the whole line length. For one far-end piston position, the received pattern is shown as the upper trace in Fig. 19. As the piston is moved, the center depressed part of the trace gradually

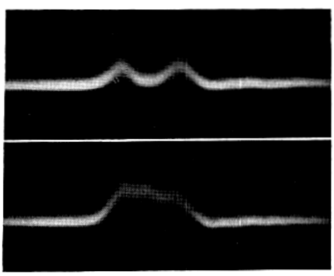

Fig. 19 — Received pulse patterns with the arrangement of Fig. 18 used for studying conversion to the TE_{31} mode.

rises until the pattern shown in the lower trace is seen. As the piston is moved farther in the same direction the trace gradually changes to have the appearance of the upper photo again. Moving the far-end piston changes the phase of energy on the return trip, and thus it can be made to add to, or nearly cancel out, conversion components that originated ahead of the piston. When the time separation becomes great enough to prevent overlapping in the pulse width, phasing effects cannot take place, therefore, the beginning and end of the spread-out received pulse are not affected by moving the piston. Energy converted at the sending end of the guide travels the full round trip to the piston and back in the slower TE_{31} mode, and thus appears at the latest time, which is at the right-hand end of the received pulse. Conversion at the piston end returns at the center of the pulse, and conversion on the return trip comes at earlier times, at the left-hand part of the pulse. The TE_{01} mode has less loss in the guide than the TE_{31} mode. Since the energy in the earlier part of the received pulse spent a greater part of the trip in the lower loss TE_{01} mode before conversion, the output is higher here, and slopes off toward the right, where the later returning energy has gone for a longer distance in the higher loss mode. The pulse height at the maximum shows the converted energy from that part of the line to be between 30 and 35 db below the incident TE_{01} energy level over the measured bandwidth.

Measurements of mode conversion from TE_{01} to TE_{21} in these wave-guides show these same effects, and also a phasing effect as a function of frequency. The TE_{21} mode has a group velocity 2.4 per cent faster than the TE_{01} mode. For a full round trip in the guides, this is a time separation of about four pulse widths between the modes. At one frequency and one far-end piston position, the TE_{21} response shown as the top trace of Fig. 20 was obtained. Moving the far-end piston gradually changed this to the second trace from the top, and further piston motion changed it back again. This is the same kind of piston phasing effect observed in the TE_{31} mode conversion studies. The irregular top of this broadened pulse indicates fewer conversion points than for the TE_{31} mode, or phasing effects along the guide length. Since the TE_{21} mode has a higher group velocity than the TE_{01} mode, energy converted at the beginning of the guide returns at the earlier or left-hand part of the pulse, and conversions on the return trip, having traveled longer in the slower TE_{01} mode, are on the right-hand side of the pulse. This is just the reverse of the situation for the TE_{31} mode. Since the loss in the TE_{21} mode is higher than in the TE_{01} mode, the right side of this broadened pulse is higher than the left side, as the energy in the left side has gone further in the higher loss TE_{21} mode. Conversions from the piston end of the guide return in the center of the pulse, and only in this region do piston phasing effects appear. As the frequency is changed the pattern changes, until it reaches the extreme shape shown in the next-to-the-bottom trace, with this narrower pulse coming at a time corresponding to the center of the broadened pulse at the top. Further frequency change in the same direction returns the shape to that of the top traces. At the frequency giving the received pulse shown on the next-to-the-bottom trace, moving the far-end piston causes a gradual change to the shape shown on the lowest trace. This makes it appear as if the mode conversion were coming almost entirely from the part of the guide near the piston end at this frequency. The upper traces appear to show that more energy is converted at the transducer end of the waveguide at that frequency. It would seem that at certain frequencies some phase cancellation is taking place between conversion points spaced closely enough to overlap within the pulse width. At frequencies between the ones giving traces like this, the appearance is more like that shown for the TE_{31} mode on Fig. 19 except for the slope across the top of the pulse being reversed. The highest part of this TE_{21} pulse is

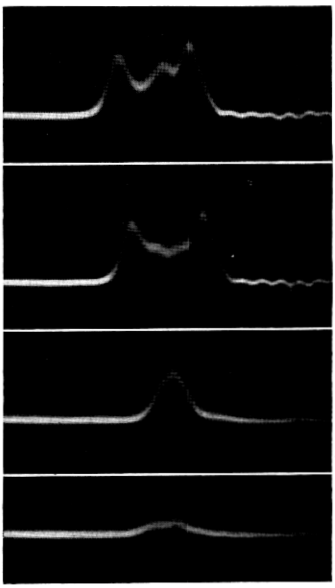

Fig. 20 — Received pulse patterns with the arrangement of Fig. 18 used for studying conversion to the TE_{21} mode.

24 to 27 db below the injected TE_{01} pulse level for the 5″ diameter Holmdel waveguides.

12. CONCLUDING REMARKS

The high resolution obtainable with this millimicrosecond pulse equipment provides information difficult to obtain by any other means. These examples of its use in waveguide investigations indicate the possibilities of the method in research, design and testing procedures. It is being used for many other similar purposes in addition to the illustrations given here, and no doubt many more uses will be found for such short pulses in the future.

REFERENCES

1. S. E. Miller and A. C. Beck, Low-loss Waveguide Transmission, Proc. I.R.E., **41**, pp. 348–358, March, 1953.
2. S. E. Miller, Waveguide As a Communication Medium, B. S. T. J., **33**, pp. 1209–1265, Nov., 1954.
3. C. C. Cutler, The Regenerative Pulse Generator, Proc. I.R.E., **43**, pp. 140–148, Feb., 1955.
4. S. E. Miller, Coupled Wave Theory and Waveguide Applications, B. S. T. J., **33**, pp. 661–719, May, 1954.